Biaxial Self-Reinforcement of Isotactic Polypropylene Prepared in Uniaxial Oscillating Stress Field by Injection Molding. II. Morphology

LI-MIN CHEN, KAIZHI SHEN

Department of Polymer Science and Engineering, Sichuan University, Chengdu, Sichuan 610065, People's Republic of China

Received 26 June 1999; accepted 15 February 2000

ABSTRACT: Scanning electron microscopy (SEM) and wide-angle x-ray diffraction (WAXD) are employed to investigate the morphology and crystallinity of isotactic polypropylene (iPP) by conventional injection molding (CIM) and oscillating packing IM (OPIM). SEM micrographs following permanganic etching show an interlocking shish-kebab morphology within the outer shear region and a much smaller spherulitic core region of the pronounced biaxially self-reinforced iPP specimen by OPIM. The OPIM moldings exhibit three crystalline forms: α, β, and γ phases. The X-ray diffraction indicates the highest α-phase orientation and largest proportion of β-phase content in the outer shear region of the OPIM moldings. © 2000 John Wiley & Sons, Inc. J Appl Polym Sci 78: 1911–1917, 2000

Key words: isotactic polypropylene; oscillating packing injection molding; biaxial self-reinforcement; permanganic etching; interlocking shish-kebab morphology

INTRODUCTION

Conventional injection-molded isotactic polypropylene (iPP) features a distinct skin–core structure, and the mechanical properties vary with the thickness of the skin layer. Kantz et al.[1] reported that the injection-molded iPP displays three layers: a highly oriented nonspherulitic skin, a shear-nucleated spherulitic intermediate layer, and a spherulitic core. Fujiyama and Wakino[2] reported that lamellae in the skin layer of injection-molded iPP are perpendicular and parallel to the injection direction and that crystallites exist with a high melting temperature and high strength, showing the characteristics of the shish-kebab morphology. Recently, Kalay and Bevis[3] gathered microstructural evidence for the presence of a shish-kebab morphology in the shear region of the conventional injection-molded iPP (their fig. 25). Our previous research[4] on self-reinforced iPP by oscillating packing injection molding (OPIM) revealed that the more perfect spherulites and the production of shish-kebab crystals in the OPIM moldings improve their mechanical properties.

In the preceding article, we achieved biaxially self-reinforced iPP by OPIM under some specific processing conditions.[5] This article concentrates on the morphologies of the iPP moldings.

EXPERIMENTAL

Material

The study material is general injection grade iPP homopolymer (1300, Yanshan Petrochemical

Correspondence to: L.-M. Chen (polymerlmchen@yahoo.com).

Contract grant sponsor: National Natural Science Foundation of China.

Journal of Applied Polymer Science, Vol. 78, 1911–1917 (2000)

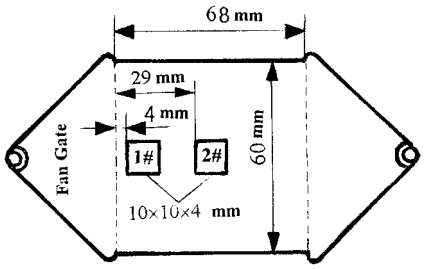

Figure 1 The positions of samples from the OPIM plate for SEM and WAXD experiments.

Corp.) with a melt flow index of 1.1 g/10 min measured at 230°C under 2.16 kg according to ASTM D1238.

Injection Molding

The test specimens were prepared by conventional IM (CIM) and OPIM according to the processing conditions described in detail in our preceding article.[5]

Scanning Electron Microscopy (SEM)

The tensile fracture surface of OPIM moldings in the flow direction (MD) and transverse direction

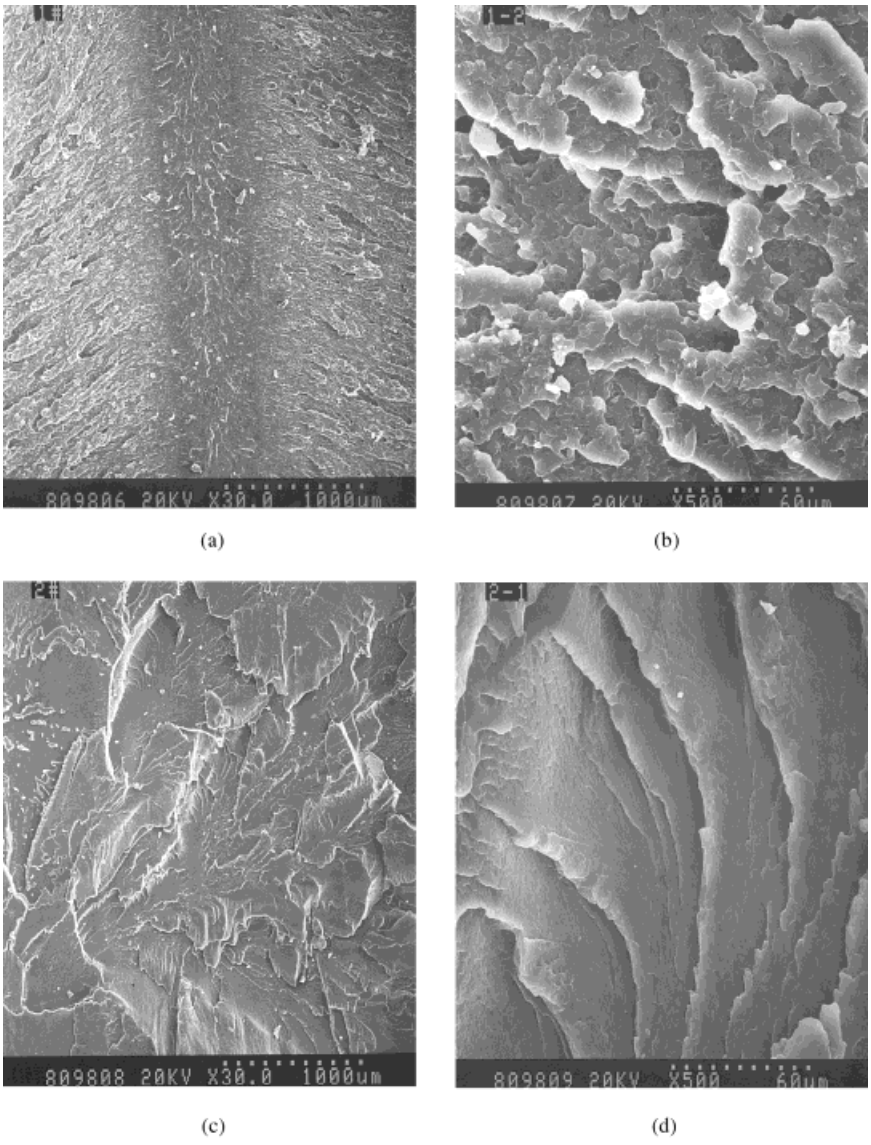

Figure 2 SEM micrographs of the tensile fracture surface of OPIM 1-9 in (a, b) the MD and (c, d) the TD.

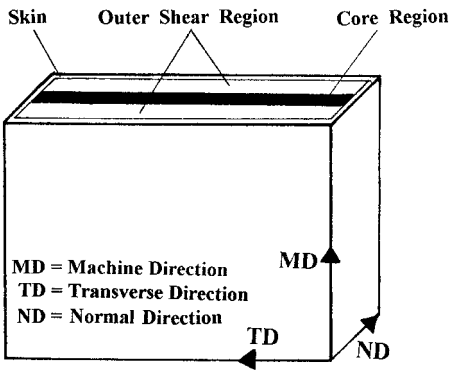

Figure 3 A schematic diagram of the reference axes and the layered structure across the section of OPIM moldings.

(TD) were examined on a Hitachi X-650 SE microscope. A thin layer of gold was evaporated on the specimens prior to the SEM observations.

The conventional injection moldings and the pronounced biaxially self-reinforced iPP specimens by OPIM were both selected for morphological studies. Square plates (10 × 10 × 4 mm) were cut from the gauge section of the conventional injection-molded tensile bars, and then the 10 × 10 mm faces were ground down to the midthickness plane (2 mm below the original surface). Square plates (10 × 10 × 4 mm) were cut out of the OPIM moldings at various positions as shown in Figure 1. Then the 10 × 10 mm faces were carefully ground and polished down to the planes with different distances from the original surface (0.1–2 mm below the original surface) until they were highly flat and smooth. All the ground and polished specimens were etched for different predetermined times using the permanganic etching technique and subsequent washing methods developed by Olley and colleagues.[6–8] Finally, the etched samples were sputtered with a very thin layer of gold and observed on a Hitachi X-650 SE microscope and an Amray 1845FE field emission microscope.

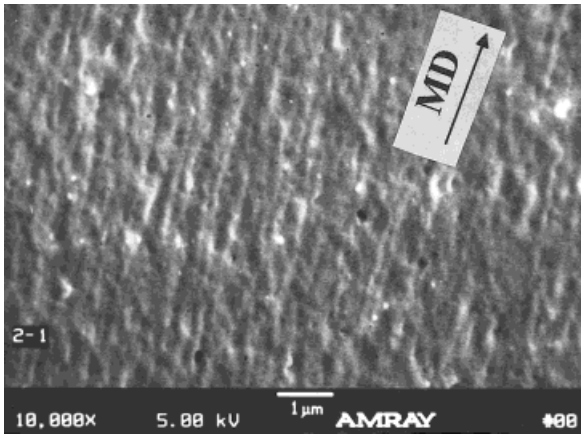

Figure 4 An SEM micrograph of the etched surface from the outer shear region of OPIM 1-9 near the fan gate.

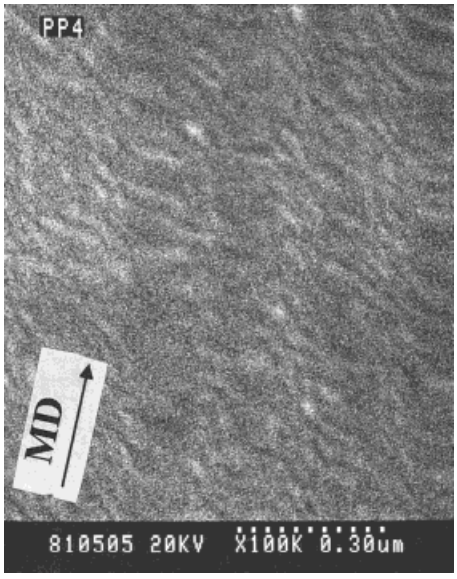

Figure 5 An SEM micrograph of the etched surface from the outer shear region of OPIM 1-9 near the center of the plate.

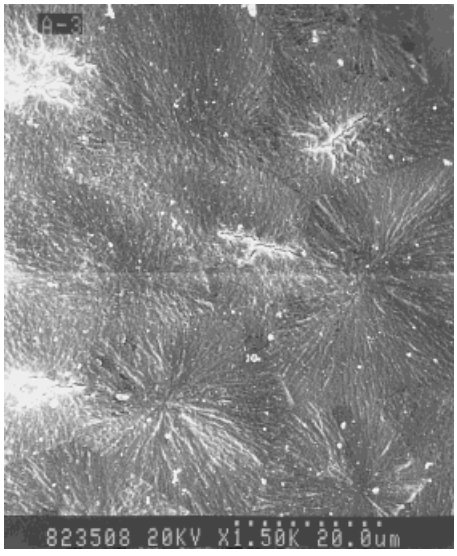

Figure 6 An SEM micrograph of the etched surface from the central core region of CIM 1.

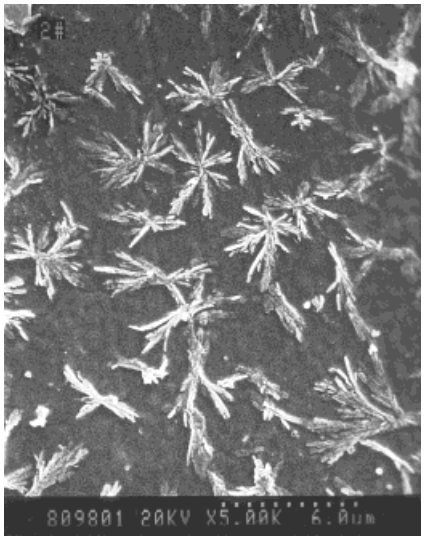

Figure 7 An SEM micrograph of the heavily etched surface from the central core region of OPIM 1-9.

Wide Angle X-Ray Diffraction (WAXD)

The specimens were cut out of the OPIM plates at the central position of 2# in Figure 1 either near the midthickness plane or near the surface. The specimens were also cut from the gauge section of the CIM tensile bars. All the specimens were used in the WAXD experiments on a D/MAX-IIIA X-ray diffractometer.

RESULTS AND DISCUSSION

The SE micrographs of the tensile fracture surface of OPIM 1-9, one of the pronounced biaxially self-reinforced iPP specimens, are shown in Figure 2. Figure 2(a) shows the fractograph of the OPIM 1-9 molding in the MD, which displays three distinct layers: two outer shear regions (each about 1.5 mm in thickness) and a core region (about 0.8 mm in thickness). Figure 3 is a schematic diagram of the layered structure across the section of OPIM moldings by further observations. A higher magnification SEM fractograph of the outer shear region illustrates a very rough and uneven failure surface with voids and crazes as shown in Figure 2(b). Figure 2(c) shows the tensile fracture surface of OPIM 1-9 in the TD,

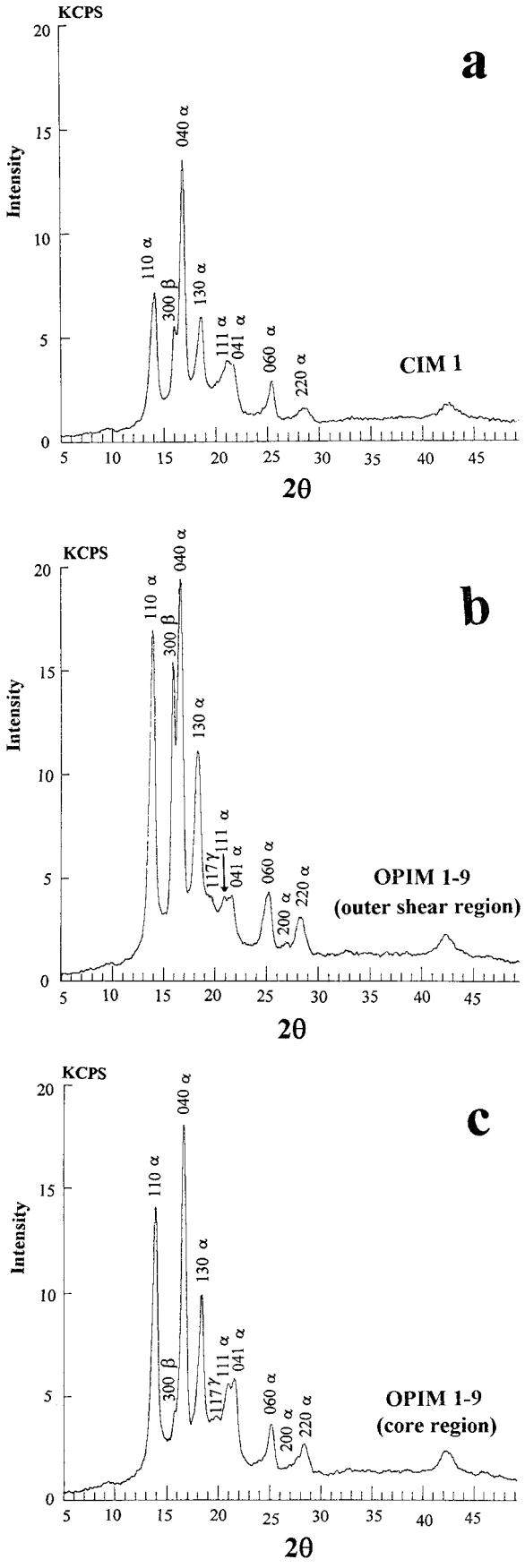

Figure 8 X-ray diffraction profiles from (a) CIM 1, (b) the outer shear region, and (c) the core region of OPIM 1-9.

Table I X-Ray Results for CIM 1

2θ (°)	d-Spacing (Å)	Miller Indices (HKL)	Crystal Phase	β-Phase Index	α-Phase Orientation Index
14.097	6.275	110	α	0.126	0.541
16.055	5.515	300	β		
16.883	5.245	040	α		
18.552	4.777	130	α		
21.185	4.131	111	α		
21.806	4.071	041	α		
25.403	3.502	060	α		
28.632	3.114	220	α		
42.469	2.126	113	α		

which exhibits a relatively planar failure surface but with delamination [Fig. 2(d)]. The evidence for the relatively ductile failure in the MD and the relatively brittle failure in the TD of the OPIM 1-9 iPP plate is consistent with the stress–strain behavior as shown in the preceding article.[5] So the failure mechanism for the OPIM 1-9 plate is quite different in the MD and TD, implying the occurrence of an anisotropic microstructure in the OPIM specimens.

In this study, permanganic etching and SEM were used to reveal the microstructure of CIMs and OPIMs. Kalay and Bevis[3] presented the experimental evidence for the shish-kebab morphol-

Table II X-Ray Results for OPIM 1-9

Sample	2θ (°)	d-Spacing (Å)	Miller Indices (HKL)	Crystal Phase	β-Phase Index	α-Phase Orientation Index
Outer shear region	13.864	6.380	110	α (+γ)	0.246	0.832
	16.043	5.520	300	β		
	16.531	5.356	040	α (+γ)		
	18.274	4.849	130	α		
	19.683	4.505	117	γ		
	21.169	4.192	111	α (+γ)		
	21.427	4.142	041	α (+γ)		
	25.069	3.548	060	α		
	26.715	3.333	200	α		
	28.243	3.156	220	α		
	42.281	2.135	113	α		
Core region	13.918	6.355	110	α (+γ)	0.032	0.621
	16.045	5.518	300	β		
	16.715	5.298	040	α (+γ)		
	18.404	4.815	130	α		
	20.038	4.426	117	γ		
	21.169	4.192	111	α (+γ)		
	21.508	4.127	041	α (+γ)		
	25.255	3.522	060	α		
	27.104	3.286	200	α		
	28.486	3.130	220	α		
	42.371	2.131	113	α		

ogy in the shear region of conventional injection-molded iPP (their fig. 25). The etched surface from the outer shear region of the sample prepared near the thickened fan gate (1# in Fig. 1) depicts fibrillar crystals aligned parallel to the MD as shown in Figure 4. This structure is considered to be induced by elongational flow near the fan gates or the coaction of both elongational and shear flow. Figure 5 is the high magnification SE micrograph of the etched surface from the outer shear region of the samples prepared near the center of the plate (2# in Fig. 1). This micrograph shows that the interpenetrating lamellae, which are perpendicular to the MD, are stacked up in the form of columns along the MD. Considering the model that Fujiyama and Wakino[2] proposed and Kalay and Bevis[3] proved, we may regard the nature of these lamellar overgrowths as a shish-kebab structure. Odell et al.[9–14] carried out extensive studies on high modulus melt-processed polyethylene filaments with an interlocking shish-kebab morphology (i.e., the zip fastener structure). They stated that this complex morphology allows the possibility of obtaining high modulus and strength without compromising the transverse properties, toughness, and creep resistance.[14] This model of interlocking shish-kebab morphology may perhaps be assumed here for the biaxial self-reinforcement of iPP in the uniaxial oscillating stress field. Evidently, the enhancement of mechanical properties in the MD of the OPIM 1-9 iPP plate may be mainly attributed to the orientation of shish-kebabs along the MD.[3,4] The effect of interlocking wedges, together with the possibility of tie molecules between lamellae of adjacent shish-kebabs, removes the weakness inherent in the column boundaries of fibrillar material[9] and improving the mechanical properties in the TD of the OPIM 1-9 iPP plate. So the tensile strength in the TD is higher than CIM but lower than that in the MD.

Figure 6 illustrates spherulites (20–30 μm diameters) in the central core region of CIM 1 after etching. Figure 6 also shows that some microcracks exist in the iPP spherulites. A spherulitic morphology in the central core region of OPIM 1-9 after heavy etching is shown in Figure 7. A comparison of these micrographs reveals that the applied oscillating stress field in the central region of OPIM moldings leads to a substantial decrease in the size of the spherulites, which also contributes to the improvement of the mechanical properties of OPIM moldings.

The X-ray diffraction profiles from CIM 1, the outer shear region, and the core region of the OPIM 1-9 plate are displayed in Figure 8(a–c), respectively. The results of the WAXD experiments indicate that the crystalline fraction in the CIM 1 molding contains α and β forms; the outer shear and core regions of OPIM 1-9 exhibit α, β, and γ phases. The α-phase orientation index and β-phase index of CIM and OPIM moldings were calculated by using the methods of Turner-Jones et al.[15] and Kalay et al.[16] Tables I and II summarize the measurements of 2θ angles, d-spacing, crystal phase, the Miller indices, α-phase orientation index, and β-phase index of samples from CIM 1, the outer shear region, and the core region of OPIM 1-9. Figure 8(b) shows the highest intensities of {110}, {040}, and {130} α-phase reflection and {300} β-phase reflection. Table II indicates the highest α-phase orientation index and the highest β-phase index in the outer shear region of OPIM 1-9. The core region of OPIM 1-9, in which the melt temperature is much higher, exhibits the lowest β-phase content in Figure 8(c) and Table II. These results are consistent with the conclusions that the tendency for β-phase formation in iPP injection moldings is high in the shear region[17] and at low melt temperature.[16,18,19]

CONCLUSIONS

The iPP prepared by OPIM displays a layered structure of a skin layer, an outer shear region, and a core region. Morphological studies and the proposed model show that the interlocking shish-kebab morphology within the outer shear region and the much smaller spherulitic core region of the OPIM moldings are induced by the action of shear to the solidifying melt. The biaxial self-reinforcement of OPIM moldings in a uniaxial oscillating stress field contributes to such morphologies. The OPIM moldings exhibit α, β, and γ phases whereas CIM moldings contain only α and β phases. The highest α-phase orientation and the largest proportion of β-phase content can be obtained in the outer shear region of OPIM moldings.

REFERENCES

1. Kantz, M. R.; Newman, H. D., Jr.; Stigale, H. J Appl Polym Sci 1972, 16, 1249.

2. Fujiyama, M.; Wakino, T. J Appl Polym Sci 1988, 35, 29.
3. Kalay, G.; Bevis, M. J. J Polym Sci Polym Phys Ed 1997, 35, 265.
4. Guan, Q.; Zhu, X.; Chiu, D.; Shen, K.; Lai, F. S.; Mccarthy, S. P. J Appl Polym Sci 1996, 62, 755.
5. Chen, L.-M.; Shen, K. J Appl Polym Sci, to appear.
6. Olley, R. H.; Hodge, A. M.; Bassett, D. C. J Polym Sci Polym Phys Ed 1979, 17, 627.
7. Olley, R. H.; Bassett, D. C. Polymer 1982, 23, 1707.
8. Bassett, D. C.; Olley, R. H. Polymer 1984, 25, 935.
9. Odell, J. A.; Grubb, D. T.; Keller, A. Polymer 1978, 19, 617.
10. Odell, J. A.; Grubb, D. T.; Keller, A. Polym Eng Sci 1979, 19, 433.
11. Bashir, Z.; Odell, J. A.; Keller, A. J Mater Sci 1984, 19, 3713.
12. Bashir, Z.; Odell, J. A.; Keller, A. J Mater Sci 1986, 21, 3993.
13. Bashir, Z.; Keller, A. Colloid Polym Sci 1989, 267, 116.
14. Bashir, Z.; Odell, J. A. J Mater Sci 1993, 28, 1081.
15. Turner-Jones, A.; Aizlewood, J. M.; Beckett, D. R. Makromol Chem 1964, 75, 134.
16. Kalay, G.; Allan, P. S.; Bevis, M. J. Plast Rubber Compos Process Applic 1995, 23, 71.
17. Dragaun, H.; Hubeny, H.; Muschik, H. J Polym Sci Polym Phys Ed 1977, 15, 1779.
18. Fleischmann, E.; Zipper, P.; Janosi, A.; Geymayer, W.; Koppelmann, J.; Schurz, J. Polym Eng Sci 1989, 29, 835.
19. Wenig, W.; Herzog, F. J Appl Polym Sci 1993, 50, 2163.